

Mechanics of actomyosin bonds in different nucleotide states are tuned to muscle contraction

Bin Guo and William H. Guilford[†]

Department of Biomedical Engineering, University of Virginia, Box 800759, Charlottesville, VA 22908

Edited by James A. Spudich, Stanford University School of Medicine, Stanford, CA, and approved May 15, 2006 (received for review February 14, 2006)

Muscle contraction and many other cell movements are driven by cyclic interactions between actin filaments and the motor enzyme myosin. Conformational changes in the actin–myosin binding interface occur in concert with the binding of ATP, binding to actin, and loss of hydrolytic by-products, but the effects of these conformational changes on the strength of the actomyosin bond are unknown. The force-dependent kinetics of the actomyosin bond may be particularly important at high loads, where myosin may detach from actin before achieving its full power stroke. Here we show that over a physiological range of rapidly applied loads, actomyosin behaves as a “catch” bond, characterized by increasing lifetimes with increasing loads up to a maximum at ≈ 6 pN. Surprisingly, we found that the myosin–ADP bond is possessed of longer lifetimes under load than rigor bonds, although the load at which bond lifetime is maximal remains unchanged. We also found that actomyosin bond lifetime is ultimately dependent not only on load, but loading history as well. These data suggest a complex relationship between the rate of actomyosin dissociation and muscle force and shortening velocity. The 6-pN load for maximum bond lifetime is near the force generated by a single myosin molecule during isometric contraction. This raises the possibility that all catch bonds between load-bearing molecules are “mechanokinetically” tuned to their physiological environment.

catch bonds | dynamic force spectroscopy | laser trap | myosin

The crystal structure of the myosin head (S1) (1) reveals how small-scale conformational changes within the hydrolytic site are converted into relatively large-scale changes producing movement. A globular “motor domain” occupies the bulk of the structure and contains both the nucleotide- and actin-binding sites (see Fig. 1). Of particular note is an α -helical extension of the heavy chain, or “neck,” protruding from the globular motor domain that acts as a rigid “lever arm” to amplify small movements arising in the nucleotide-binding pocket (2–5). Concomitant with phosphate release, rotation of the neck causes a step of an ≈ 5.5 -nm “working stroke” and an isometric force of 0.7–9 pN (3, 6–10) that has been the subject of numerous single-molecule mechanics studies.

Another feature of particular note within the motor domain is a cleft that divides the actin-binding site (2). This cleft is thought to close upon binding to actin (1, 2, 11–13), bringing into position residues on both sides of the cleft that are involved in strong binding to actin: the so-called R-site and A-site. Evidence suggests that there may be additional conformational changes in the actin-binding interface that accompany ADP release. The cleft at the actin-binding interface of smooth muscle myosin may close further upon ADP release (14, 15) and is accompanied by an increase in R-site flexibility (14, 16). Thus, although both the R-site and A-site are tightly bound to actin in the presence of ADP, upon ADP release from smooth muscle myosin the R-site adopts a more flexible conformation whereas the A-site remains tightly bound. EM reconstructions reveal no similar closure of the cleft in skeletal muscle myosin upon ADP release, although the resolution of the technique was limited. It does appear, however, that there are increases in R-site flexibility in skeletal muscle myosin upon ADP release (14).

Although invaluable to our understanding of myosin function, neither technique sheds light on the biophysical consequences of changes in shape at the actin-binding interface of myosin. The mechanical consequences are especially critical given that the actomyosin bond is designed to operate under load. Although some work has been done to measure the “strength” of the rigor bond to actin (17–19), little is known about the response of the actin–myosin bond to load in well defined geometries and under physiological loading histories. Nothing is known about how the strength of actomyosin bonds changes between discrete nucleotide bound states or between myosin isoforms. Nor is it known how bond duration relates to overall myosin function during contraction. However, the observation that at high loads the actomyosin bond may dissociate before the power stroke reaches its maximum deflection (20) highlights its importance.

To test the hypothesis that a conformational change in the actin-binding interface of skeletal muscle myosin accompanies ADP release, and to gain a clear understanding of the functional consequences of that putative change, we measured the load-dependent kinetics (energy landscapes) of myosin unbinding from actin in both the rigor and ADP states. A laser trap was used to apply loads to single actomyosin bonds either “instantaneously” or as linearly increasing loads over time. Bond lifetime and bond rupture force were subsequently measured. We found that over a physiological range of rapidly applied loads, actomyosin behaves as a “catch” bond, characterized by increasing lifetimes with increasing loads up to a maximum at ≈ 6 pN. The catch bond behavior converted to apparent slip bond behavior in a force history-dependent fashion similar to selectin bonds (21). Surprisingly, we found that the myosin–ADP bond is possessed of longer lifetimes under load than rigor bonds, although the load at which bond lifetime is maximal remains unchanged. These data support the hypothesis that the skeletal actomyosin bond changes conformation upon ADP release. The close correspondence between the 6-pN load for maximum bond lifetime and the isometric force generated by a single myosin molecule suggests the actomyosin bond may be “tuned” to contraction.

Results

The Skeletal Actomyosin Bond Changes Between the ADP and Rigor States.

Rat skeletal actomyosin bond rupture force was first measured over ≈ 3 orders of magnitude range of loading rates. A laser trap was used to hold an actin-coated bead against the side of a skeletal heavy meromyosin (HMM)-coated target (Fig. 2A), and the target moved away from the laser trap over a range of velocities. Higher velocities (v) at a given trap stiffness (α) resulted in higher loading rates ($r_f = v\alpha$). Bond lifetime and rupture force were measured in both the ADP and rigor states over a range of loading rates. As expected, they were loading rate

Conflict of interest statement: No conflicts declared.

This paper was submitted directly (Track II) to the PNAS office.

Abbreviation: HMM, heavy meromyosin.

[†]To whom correspondence should be addressed. E-mail: guilford@virginia.edu.

© 2006 by The National Academy of Sciences of the USA

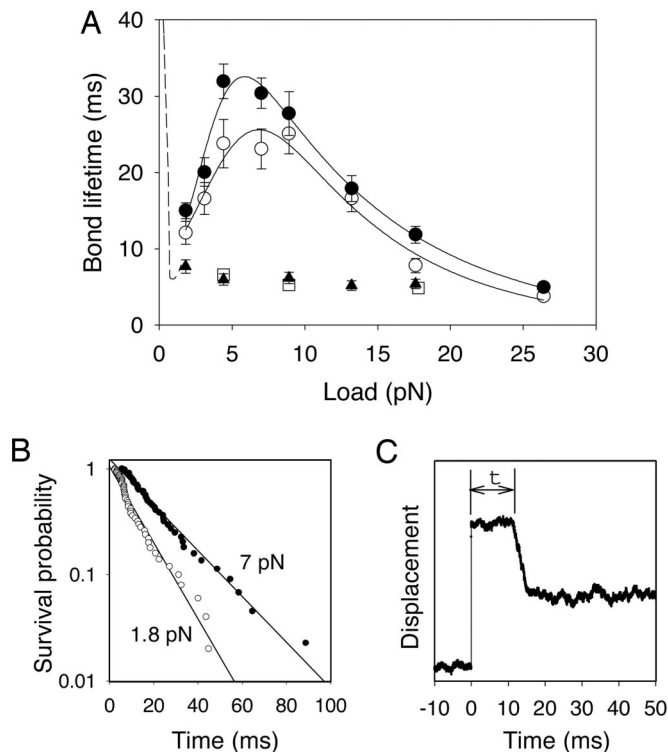


Fig. 4. Catch-slip behavior in actomyosin bonds. (A) Actomyosin-ADP bonds (●) appear to be stronger than rigor bonds (○), and both states demonstrate the catch-slip behavior illustrated in Fig. 2B. Corresponding data taken in the presence of PP_i (▲) are superimposed. Control data (◻) were collected in the presence of HMM but without actin on the beads. Error bars represent SEM. (B) Bond survival curves at two discrete forces demonstrate single exponential decays ($n = 50$ in each case). (C) Example raw data trace showing the onset of a loading step at time 0. A bond results in the bead remaining displaced from trap center for a period t (the bond lifetime). Bond rupture allows the bead to return to a new baseline. The baselines before and after the step are slightly offset because of an optical artifact when the trapped bead is positioned against the target bead (see text).

quency of bond formation. In contrast, the inner barrier underwent large changes in both characteristic bond length (x_{β} , 5-fold increase) and unloaded dissociation rate (k_{off}^0 , 4-fold decrease) upon ADP loss. In other words, although the dissociation rate of the rigor actomyosin bond is lower when unloaded, it is considerably more sensitive to load than the actomyosin-ADP bond.

Data from kinesin have shown that bonds involving two heads are stronger than those involving one (29). Assuming this finding applies to actomyosin, the higher rupture force of the inner barrier in the ADP state relative to rigor may be explained by both heads binding to actin in the ADP state and one head dissociating from actin in rigor. To address this possibility, single-headed HMM bond lifetimes in the two states were measured at key loading rates. The data for both the rigor and ADP states superimpose with the two-headed data (Fig. 3), refuting this hypothesis. Values for the outer barrier in rigor are similar to those reported by Nishizaka *et al.* (17) for single-headed binding in the only comparable study of these phenomena.

Actomyosin Is a Catch Bond That Is Stronger in the ADP State than in Rigor. Step loads (1.8–26.4 pN) were applied to acto-HMM bonds by rapidly displacing the laser trap relative to the target, and the bond lifetimes were measured at both the rigor and ADP states. As demonstrated in Fig. 4A, actomyosin bond lifetimes increase with increasing load up to a maximum at ≈ 6 pN, a

Table 2. Fitted Bell parameters for the slip and catch two-pathway model

State	Slip pathway		Catch pathway	
	k_{off}^0 , s^{-1}	x_{β} , nm	k_{off}^0 , s^{-1}	x_{β} , nm
Rigor	13 ± 5	0.5 ± 0.1	127 ± 43	-1.5 ± 0.6
ADP	15 ± 2	0.40 ± 0.05	176 ± 62	-2.5 ± 0.6

behavior known as a catch bond (Fig. 2B) (23). Above 6 pN, bond lifetimes decrease with increasing loads. Similar “catch-slip” behavior, with first increasing and then decreasing bond lifetimes, has been observed by others in selectin-PSGL-1 bonds (30, 31). Bond lifetimes in the ADP state were 24% longer than that in the rigor state at the optimal load.

There are several published models describing the catch-slip behavior observed here (32–35). We fit the data as a single bound state and two parallel pathways to bond dissociation (35). Interpreted within this model, bond lifetime is determined by competition between two parallel dissociation pathways. One pathway (slip) is “slow” and increases only slowly in response to imposed loads. The other (catch) is very fast but becomes rapidly slower in response to imposed loads. This model is represented by the equation $1/\tau_{\text{on}} = k_{\text{off}}^0 e^{f x_{\text{c}}/k_{\text{BT}}} + k_{\text{off}}^0 e^{f x_{\text{s}}/k_{\text{BT}}}$, which is the sum of two Bell models. Subscripts c and s indicate the catch and slip pathways, respectively, and τ_{on} is the mean bond lifetime. Lifetime is maximal at the critical force, f_{crit} , which is similar for ADP and rigor (6.4 and 7.1 pN, respectively). The slip pathway does not differ between the ADP and rigor states (Table 2). The catch pathway, in contrast, has a 50% higher unloaded dissociation rate and an effective 3-fold increased sensitivity to load ($e^{x_{\text{c}}/k_{\text{BT}}}/e^{x_{\text{c}}/k_{\text{BT}}}$) in the ADP state relative to rigor.

The same measurement was performed in the presence of 1 mM Na₄P₂O₇ (pyrophosphate; PP_i), which is thought to be analogous to the prehydrolysis, myosin-ATP state (36). As expected, the measured lifetimes were much shorter than for rigor and ADP states at any given load and were load independent. Although the measured lifetimes in the PP_i state were indistinguishable from actin-free controls, the binding frequency with PP_i was much higher than control, suggesting the interactions in the presence of PP_i were weak but specific between myosin and actin.

To determine the bond lifetimes in the same physical system but at near-zero load, an actin-coated bead was captured and placed adjacent to the HMM-coated surface in the presence and absence of ADP. Bonds were allowed to form and break with low, semirandom loads ultimately determined by the separation distance between trap center and the bound position of the microsphere. Bond lifetime was measured by a small baseline shift and reduction in Brownian motion. The trap stiffness and detector sensitivity were both altered in close proximity to the target. Thus, fits to power spectral density were used to calibrate the laser trap in that position. The average measured load was 0.07 ± 0.01 pN, and lifetimes for rigor and ADP states under this load were 3.8 ± 0.7 and 2.7 ± 0.7 s, respectively. Experiments with control beads yielded no such interactions. These data are consistent with solution studies where it has been shown that the bond lifetime in the rigor state is longer than that in the ADP state (37).

Lifetime of the Actomyosin Bond Is Loading History-Dependent. As mentioned earlier, there are several models describing catch-slip behavior. Most of these models predict the unbinding rate to depend only on the instantaneous load (34, 35) and not on loading history. One thus should be able to predict our loading rate vs. rupture force data based on our instantaneous load data. We thus assumed the inverse mean bond lifetime $1/\tau_{\text{on}}$ as

equivalent to $k_{\text{off}}(f)$. Based on these measures of $k_{\text{off}}(f)$, we performed stochastic simulations to predict the characteristic rupture forces at various loading rates. The predicted rupture forces consistently underestimate the measured rupture force by ≈ 5 -fold (Fig. 3, dashed line) in rigor. This result demonstrates that the actomyosin bond is sensitive to loading history as well as absolute load, similar to the response of selectin–PSGL-1 bonds (21, 32).

A recent “allosteric catch bond” model suggests that a bound molecule may switch at a load-dependent rate between two conformations with different dissociation rates (33). This model would allow for history dependence. However, this model also predicts that at any given load one would observe a double-exponential decay over time of the bound fraction of molecules. The bound fraction of actomyosin at a variety of loads were distributed as a single exponential (Fig. 4B), which appears to eliminate the allosteric model as describing actomyosin interactions. Thus, an analytical description of history dependence in actomyosin bonds is lacking and requires further study.

Discussion

Our data suggest a significant conformational change in the actin-binding interface of skeletal muscle myosin upon ADP release. This conformational change results in a “weaker” bond in the rigor state, contrary to the traditional view from solution kinetics studies. As stated earlier, myosin initially binds to actin via both sides of the actin binding cleft, namely at the A- and R-sites. Experimental evidence suggests a more flexible and perhaps more loosely bound R-site in the rigor state when compared with the ADP state (14, 16) and may account for the differences observed here. A longer-duration bond while ADP remains bound to myosin makes intuitive sense. Rigor can be thought of as a transitional state before binding of ATP, which takes place on the scale of <1 ms at physiological [ATP]. The rate of ADP release from myosin then becomes the limiting step in determining how long myosin tends to remain attached to actin (38). A longer-lasting actomyosin–ADP bond therefore may be appropriately tuned to match the duration of this strongly bound state. This quality is in contrast to the rigor bond, which may rupture physiologically under high load (20).

Some myosins, including smooth muscle myosin, undergo a second power stroke upon ADP release (39). Evidence suggests that imposed loads capture ADP within the nucleotide-binding site of myosin by opposing this conformational change and thus extend the attached lifetime (39). This hypothesis has been proposed as an explanation for the “latch” state of smooth muscle (39) and for interhead coordination in processive myosins (40–42). Recently a small ADP release-associated powerstroke was observed in skeletal muscle myosin (43), suggesting that in striated myosins too imposed loads may extend the duration of the actomyosin–ADP state.

Catch bonds may be of use in extending the lifetime of the actomyosin complex under load. While applying instantaneous (step) loads to the actomyosin bond, the bond lifetime first increases with increasing load, as characterized by a catch bond, and then decreases with increasing load after reaching a maximum at ≈ 6 pN. Imposed loads thus may give rise not only to longer-lived strong-binding states (actomyosin and actomyosin–ADP) but to a proportionately increased actomyosin bond lifetime. Myosins with larger power strokes associated with ADP release might therefore be expected to demonstrate even larger differences than those observed here in the durations of the rigor and actomyosin–ADP bonds when under load. Force spectroscopy of smooth muscle and processive myosins, both of which have large second power strokes and highly load-sensitive rates of ADP release, will test this hypothesis.

The value 6 pN is close to or slightly above the isometric force a single myosin exerts on an actin filament during a power stroke

(6, 8, 10). If we assume that the force generating conformational change in myosin occurs on a short timescale [<1 ms, the upper limit set by laser trap studies (6–8)], then step loads are the relevant loading paradigm during force generation in myocytes. Because step loads result in catch behavior, catch is the relevant physiological behavior of the actomyosin bond. The close correspondence between the critical force of the bond and the unitary force of myosin suggests the bond is “mechanokinetically” tuned to its physiological application; that is, the lifetime of the actomyosin bond is longest when myosin is generating its peak isometric force. It is tempting to speculate that all catch bonds are mechanokinetically tuned to better perform their functions. If so, then the measured critical force of catch–slip transition is a valuable indicator of the maximum physiological load experienced by the molecule: ≈ 25 pN for L-selectin–PSGL-1 bonds (30) and ≈ 30 pN for bacterial FimH–mannose bonds (33). This theory may prove useful, because the load experienced by most adhesion molecules *in vivo* cannot currently be directly measured.

These data also may provide an explanation for the disparate unitary displacements measured for myosin in different laboratories. Studies using native myosin or HMM bound to the motility surface through antibodies generally measure unitary steps of 10 nm (3, 6, 8), whereas those using S1, single-headed HMM, or HMM bound directly to glass or nitrocellulose generally measure steps of 5 nm (7, 9). The simple explanation is that HMM has little left resembling the long tail of myosin and therefore is obligated to bind to the motility surface by one head, disabling it. Indeed, our single-headed HMM data imply that under our experimental conditions HMM binds to actin with only one head whether or not both heads are present, consistent with reports (44). Further, we found that when an equimolar concentration of HMM was applied to flow cells, the measured surface density of active heads (heads per μm^2) was $\approx 60\%$ of that when native myosin was applied. Together, these data suggest that when it is applied to a flow cell, HMM binds to the nitrocellulose surface by one head, thus losing its hydrolytic and actin-binding capabilities. One head generates 5-nm steps, whereas two heads work cooperatively to generate 10-nm steps (9, 45).

At first glance our relatively short bond lifetimes seem to be in conflict with solution studies, where rigor actomyosin bonds last ≈ 100 s (37). However, solution studies are, by definition, performed at zero load and need not be representative of mechanically loaded physiological conditions. We mimicked solution conditions by imposing very low, 0.07-pN loads and indeed found that bond lifetimes were orders of magnitude higher under these conditions (Fig. 4A, dashed line). This finding suggests that the unusually large drop in bond lifetime under piconewton loads is real and not an artifact of our experimental system. Interpreting these low-load data is nonetheless difficult. We fit a Bell-type slip bond model to our lowest force data points (0.07 and 1.8 pN) as well as the dissociation rate at zero force in solution (0.01 s^{-1}) and estimated a characteristic bond length (x_{β}) of 15 nm. This value is on the length scale of the myosin motor domain and probably is not physically realizable. Thus, an interesting question is how actomyosin comes to have an unreasonably low apparent dissociation rate when unloaded. One possible explanation is rapid, weak rebinding of the myosin head to actin. Measuring the lifetime of the loaded actomyosin bond at physiological ionic strength may help resolve this issue.

As shown in Fig. 2A, we applied loads to actomyosin bond perpendicular to the major axis of actin. Thus, although our absolute measures of rupture force and bond lifetime are not necessarily representative of that in intact muscle where loads are parallel to the actin filament, we nonetheless demonstrate a relative change in the actomyosin bond mechanics in the ADP and rigor states. This finding supports the hypothesis that a

conformational change in the skeletal actomyosin interface accompanies ADP release. Further, the geometry of force application in our experiments is known and well controlled. In fact, the actomyosin bond will offer exciting new opportunities for bond mechanics study because methods are available for applying loads to the bond both perpendicular and parallel to the actin filament axis. The “three-bead” assay in which an actin filament is suspended between two laser traps (6) will allow the latter experiment. Such variations in the geometry of force application have not been possible for other catch-slip bonds, such as selectins and FimH, which are not filamentous and would prove difficult to orient. Loads applied in multiple, defined geometries should prove informative in understanding the influence of directional forces on biological bonds.

Our data do not agree in all respects with the only published study of actomyosin bond behavior under step loads (17). Our measured lifetimes are considerably shorter by comparison. That our rupture forces under constant rates of load compare favorably with work from the same group (19) suggests that there are no major biological differences. However, there are several differences in experimental technique that could account for the discrepancy. First, we attached HMM to a nitrocellulose-coated surface, whereas Nishizaka *et al.* (17) attached HMM to a silanized glass surface. Different surfaces potentially alter HMM adsorption, giving rise to conformational differences in the molecules or simply different orientations of the globular heads. This point of view is supported by changes in actin filament velocity when propelled by myosin adhered to different motility surfaces (46–48). Second, as just described, we applied loads to single actomyosin bonds perpendicular to the actin axis, whereas Nishizaka *et al.* (17) applied loads along the actin filament. Although more physiological in geometry, Nishizaka *et al.* (17) pointed out that their actin was attached to multiple HMM molecules and with an unknown degree of slack in the actin filament. As a result, there may have been load sharing between multiple HMM molecules. Load sharing may have lengthened the measured bond lifetimes considerably. Finally, Nishizaka *et al.* (17) applied step loads by moving a piezoelectric stage, which is limited in speed. As we have demonstrated, actomyosin bond lifetimes are load history dependent. Under slowly applied loads, lifetimes are disproportionately longer than those under comparatively instantaneous loads.

The dissociation rate of the actomyosin bond was postulated to be a function of strain in the early models of A. F. Huxley (49). The present work supports that basic assumption but points to a complex relationship between load and bond lifetime. Adding to the complexity, the dissociation rate of the actomyosin bond is a function not only of instantaneous load but also of loading history. This phenomenon could have dramatic implications for all of the force-dependent steps in the crossbridge cycle. Along with the lifetime of the actomyosin bond itself, transitions between nucleotide-binding states might depend not only on force but also on shortening velocity.

Methods

Proteins. Myosin and HMM were prepared from rat skeletal muscle as described (50). Single-headed HMM (sh-HMM) was prepared by papain digestion essentially as described with minor modifications (51). All proteins were stored in liquid nitrogen in 50% glycerol, if not used immediately.

F-actin was polymerized from rabbit G-actin (Cytoskeleton, Denver), stabilized by phalloidin, and then covalently coupled to 1.2 μm (diameter) carboxylated polystyrene beads (Bangs Laboratories, Fishers, IN) by using 1-ethyl-3-(3-dimethylaminopropyl)-carbodiimide hydrochloride (EDAC; Sigma). After quenching the remaining active sites on the beads in 100 mM ethanolamine (Sigma), the actin-beads were blocked with 1 mg/ml BSA to reduce nonspecific interactions. HMM was

likewise used instead of native myosin to reduce nonspecific interactions between actin and the myosin tail (50).

Laser Trap. The laser trap used in these studies has been described in detail elsewhere (52). Back focal plane interferometry (53) was used to measure the position of the trapped bead relative to the trap center, thus providing measurements of displacement and force. The interferometer and the trap stiffness were calibrated by step response method (52, 54, 55) and by fits to the power spectral density (52, 53, 55).

Nitrocellulose-coated coverslips with pedestals were prepared as described (8) by spraying a glass bead suspension onto 22 \times 22-mm coverslips and subsequently coating with nitrocellulose. These then were assembled into a 30- μl flow cell. A total of 1–2 $\mu\text{g/ml}$ rat skeletal HMM in actin buffer (25 mM KCl/25 mM imidazole/1 mM EGTA/4 mM MgCl_2 , pH 7.4) was incubated in a flow cell for 1 min at room temperature. The flow cell then was blocked with 1 mg/ml BSA for 1 min to block unbound sites on the nitrocellulose. A suspension of actin-coated beads in actin buffer then was introduced to the flow cell. An oxygen scavenger system (0.125 mg/ml glucose oxidase, 0.0225 mg/ml catalase, and 2.87 mg/ml glucose) and 10 mM DTT were included in the beads suspension. ADP at 2 mM also was included for specific experiments.

The flow cell was put onto a piezoelectric microscope stage. The bead concentration was chosen so that only a limited number of beads were present per visual field to reduce noise caused by neighboring beads and to avoid capturing multiple beads in the trap. A bead was captured in the laser trap and brought into contact with a HMM-coated glass bead on the surface (Fig. 2).

Force Spectroscopy. To apply constant loading rates to actomyosin bonds, the surface was moved away by a piezoelectric stage at a constant velocity. The bead was displaced from the trap center only if a bond had formed between the two beads. The loading rate was varied by changing the trap stiffness (0.016–0.067 pN/nm) or the rate at which the stage moved (0.18–18 nm/ms) or both. The HMM density on the surface was estimated to be ≈ 20 heads per μm^2 to ensure that we only measured single-molecule events. The assumption of single bonds is further supported by the low frequency of bond formation. Less than 1 in 20 contacts resulted in a bond.

To apply instantaneous steps in load, the trap was stepped away from the HMM-coated surface. The bond lifetime was measured by the time the bead remained bound to the HMM-coated surface (Fig. 4C). Although the transition between trap positions required only 10 μs , the rate at which load was applied was further limited by motion of the actin-coated bead in a viscous medium against the elastic load of actomyosin. Thus, the actual time it took to complete a step load was modeled assuming the actomyosin bond to be a spring of stiffness E and the trapped bead a dashpot in parallel with a spring of stiffness α . If the trap is displaced by a distance D , the governing equation is $E \cdot \varepsilon + \eta \dot{\varepsilon} = \alpha(D - \varepsilon)$, where η is the viscous damping of the trapped bead, modeled as Stokes drag on a sphere, and ε is the strain of the bonded actomyosin pair. Solving for time-dependent strain of the tether in response to a step of the laser trap we find

$$\varepsilon(t) = \frac{\alpha D}{E + \alpha} (1 - e^{-(E + \alpha)t/\eta}),$$

where D , η , and α are known. Based on an estimated elasticity of 0.7 pN/nm for skeletal actomyosin (56, 57), our steps in load were 70% complete within 30 μs . Even over a broader range of crossbridge stiffnesses from 0.13 pN/nm (44) to 2 pN/nm (58), the time to reach 70% load ranged from 15 to 40 μs and therefore was interpreted as instantaneous.

Reasonable compliances outside the actomyosin bond will not significantly alter our conclusions. Consider a moderate load of 10 pN imposed by displacing a trap of stiffness $0.037 \text{ pN} \times 270 \text{ nm}$ (typical conditions). Assuming a comparable mechanical compliance outside the actomyosin complex of 0.7 pN/nm , our actual imposed load would be diminished by only 3%.

Although it may be of concern that some bond besides the actomyosin bond ruptured during loading (e.g., myosin from surface or actin from bead), evidence is to the contrary. The loads applied here are not sufficient to break the covalent bond linking the actin filament to the microsphere. Further, repeated

“touching” of the microsphere to the myosin-coated surface continued to yield specific bonds at a constant probability. This result would not be expected if the myosin were being removed from the surface.

We thank Dr. Wendy Thomas (University of Washington) for fruitful discussions of bond mechanics and the Cardiovascular Research Center at the University of Virginia for scholarly support and encouragement. This work was supported by National Institutes of Health Grants AR45604 and HL64381 and by the Department of Biomedical Engineering (University of Virginia).

1. Rayment, I., Rypniewski, W. R., Schmidt-Base, K., Smith, R., Tomchick, D. R., Benning, M. M., Winkelmann, D. A., Wesenberg, G. & Holden, H. M. (1993) *Science* **261**, 50–58.
2. Rayment, I., Holden, H. M., Whittaker, M., Yohn, C. B., Lorenz, M., Holmes, K. C. & Milligan, R. A. (1993) *Science* **261**, 58–65.
3. Warshaw, D. M., Guilford, W. H., Freyzon, Y., Kremntsova, E., Palmiter, K. A., Tyska, M. J., Baker, J. E. & Trybus, K. M. (2000) *J. Biol. Chem.* **275**, 37167–37172.
4. Uyeda, T. Q., Abramson, P. D. & Spudich, J. A. (1996) *Proc. Natl. Acad. Sci. USA* **93**, 4459–4464.
5. Anson, M., Geeves, M. A., Kurzawa, S. E. & Manstein, D. J. (1996) *EMBO J.* **15**, 6069–6074.
6. Finer, J. T., Simmons, R. M. & Spudich, J. A. (1994) *Nature* **368**, 113–119.
7. Molloy, J. E., Burns, J. E., Kendrick-Jones, J., Tregear, R. T. & White, D. C. (1995) *Nature* **378**, 209–212.
8. Guilford, W. H., Dupuis, D. E., Kennedy, G., Wu, J., Patlak, J. B. & Warshaw, D. M. (1997) *Biophys. J.* **72**, 1006–1021.
9. Tyska, M. J., Dupuis, D. E., Guilford, W. H., Patlak, J. B., Waller, G. S., Trybus, K. M., Warshaw, D. M. & Lowey, S. (1999) *Proc. Natl. Acad. Sci. USA* **96**, 4402–4407.
10. Takagi, Y., Homsher, E. E., Goldman, Y. E. & Shuman, H. (2006) *Biophys. J.* **90**, 1295–1307.
11. Yengo, C. M., De la Cruz, E. M., Chrin, L. R., Gaffney, D. P. & Berger, C. L. (2002) *J. Biol. Chem.* **277**, 24114–24119.
12. Holmes, K. C., Angert, I., Kull, F. J., Jahn, W. & Schroder, R. R. (2003) *Nature* **425**, 423–427.
13. Volkman, N., Hanein, D., Ouyang, G., Trybus, K. M., DeRosier, D. J. & Lowey, S. (2000) *Nat. Struct. Biol.* **7**, 1147–1155.
14. Volkman, N., Ouyang, G., Trybus, K. M., DeRosier, D. J., Lowey, S. & Hanein, D. (2003) *Proc. Natl. Acad. Sci. USA* **100**, 3227–3232.
15. Xiao, M., Reifengerger, J. G., Wells, A. L., Baldacchino, C., Chen, L. Q., Ge, P., Sweeney, H. L. & Selvin, P. R. (2003) *Nat. Struct. Biol.* **10**, 402–408.
16. Yengo, C. M., Chrin, L., Rovner, A. S. & Berger, C. L. (1999) *Biochemistry* **38**, 14515–14523.
17. Nishizaka, T., Seo, R., Tadakuma, H., Kinoshita, K., Jr., & Ishiwata, S. (2000) *Biophys. J.* **79**, 962–974.
18. Nakajima, H., Kunioka, Y., Nakano, K., Shimizu, K., Seto, M. & Ando, T. (1997) *Biochem. Biophys. Res. Commun.* **234**, 178–182.
19. Nishizaka, T., Miyata, H., Yoshikawa, H., Ishiwata, S. & Kinoshita, K., Jr. (1995) *Nature* **377**, 251–254.
20. Reconditi, M., Linari, M., Lucii, L., Stewart, A., Sun, Y. B., Boesecke, P., Narayanan, T., Fischetti, R. F., Irving, T., Piazzesi, G., et al. (2004) *Nature* **428**, 578–581.
21. Marshall, B. T., Sarangapani, K. K., Lou, J., McEver, R. P. & Zhu, C. (2005) *Biophys. J.* **88**, 1458–1466.
22. Bell, G. I. (1978) *Science* **200**, 618–627.
23. Dembo, M., Torney, D. C., Saxman, K. & Hammer, D. (1988) *Proc. R. Soc. London Ser. B* **234**, 55–83.
24. Evans, E. & Ritchie, K. (1997) *Biophys. J.* **72**, 1541–1555.
25. Merkel, R., Nassoy, P., Leung, A., Ritchie, K. & Evans, E. (1999) *Nature* **397**, 50–53.
26. Yuan, C., Chen, A., Kolb, P. & Moy, V. T. (2000) *Biochemistry* **39**, 10219–10223.
27. Tees, D. F., Waugh, R. E. & Hammer, D. A. (2001) *Biophys. J.* **80**, 668–682.
28. Rinko, L. J., Lawrence, M. B. & Guilford, W. H. (2004) *Biophys. J.* **86**, 544–554.
29. Kawaguchi, K. & Ishiwata, S. (2001) *Science* **291**, 667–669.
30. Marshall, B. T., Long, M., Piper, J. W., Yago, T., McEver, R. P. & Zhu, C. (2003) *Nature* **423**, 190–193.
31. Yago, T., Wu, J., Wey, C. D., Klopocki, A. G., Zhu, C. & McEver, R. P. (2004) *J. Cell Biol.* **166**, 913–923.
32. Barsegov, V. & Thirumalai, D. (2005) *Proc. Natl. Acad. Sci. USA* **102**, 1835–1839.
33. Thomas, W. E., Forero, M., Yakovenko, O., Nilsson, L. M., Vicini, P., Sokurenko, E. V. & Vogel, V. (2006) *Biophys. J.* **90**, 753–764.
34. Evans, E., Leung, A., Heinrich, V. & Zhu, C. (2004) *Proc. Natl. Acad. Sci. USA* **101**, 11281–11286.
35. Pereverzev, Y. V., Prezhdo, O. V., Forero, M., Sokurenko, E. V. & Thomas, W. E. (2005) *Biophys. J.* **89**, 1446–1454.
36. Graeinerich, D. & Portzehl, H. (1964) *Biochim. Biophys. Acta* **86**, 567–578.
37. Marston, S. B. (1982) *Biochem. J.* **203**, 453–460.
38. Lauzon, A. M., Tyska, M. J., Rovner, A. S., Freyzon, Y., Warshaw, D. M. & Trybus, K. M. (1998) *J. Muscle Res. Cell Motil.* **19**, 825–837.
39. Veigel, C., Molloy, J. E., Schmitz, S. & Kendrick-Jones, J. (2003) *Nat. Cell Biol.* **5**, 980–986.
40. Veigel, C., Schmitz, S., Wang, F. & Sellers, J. R. (2005) *Nat. Cell Biol.* **7**, 861–869.
41. Baker, J. E., Kremntsova, E. B., Kennedy, G. G., Armstrong, A., Trybus, K. M. & Warshaw, D. M. (2004) *Proc. Natl. Acad. Sci. USA* **101**, 5542–5546.
42. Nyitrai, M. & Geeves, M. A. (2004) *Philos. Trans. R. Soc. London Ser. B* **359**, 1867–1877.
43. Capitanio, M., Canepari, M., Cacciafesta, P., Lombardi, V., Cicchi, R., Maffei, M., Pavone, F. S. & Bottinelli, R. (2006) *Proc. Natl. Acad. Sci. USA* **103**, 87–92.
44. Molloy, J. E., Burns, J. E., Sparrow, J. C., Tregear, R. T., Kendrick-Jones, J. & White, D. C. (1995) *Biophys. J.* **68**, 298S–303S.
45. Kad, N. M., Rovner, A. S., Fagnant, P. M., Joel, P. B., Kennedy, G. G., Patlak, J. B., Warshaw, D. M. & Trybus, K. M. (2003) *J. Cell Biol.* **162**, 481–488.
46. Kron, S. J. & Spudich, J. A. (1986) *Proc. Natl. Acad. Sci. USA* **83**, 6272–6276.
47. Harada, Y., Sakurada, K., Aoki, T., Thomas, D. D. & Yanagida, T. (1990) *J. Mol. Biol.* **216**, 49–68.
48. Harris, D. E. & Warshaw, D. M. (1993) *J. Biol. Chem.* **268**, 14764–14768.
49. Huxley, A. F. (1957) *Prog. Biophys. Biophys. Chem.* **7**, 255–318.
50. Guo, B. & Guilford, W. H. (2004) *Cell Motil. Cytoskeleton* **59**, 264–272.
51. Margossian, S. S. & Lowey, S. (1982) *Methods Enzymol.* **85**, 55–71.
52. Guilford, W. H., Tournas, J. A., Dascalu, D. & Watson, D. S. (2004) *Anal. Biochem.* **326**, 153–166.
53. Allersma, M. W., Gittes, F., deCastro, M. J., Stewart, R. J. & Schmidt, C. F. (1998) *Biophys. J.* **74**, 1074–1085.
54. Dupuis, D. E., Guilford, W. H., Wu, J. & Warshaw, D. M. (1997) *J. Muscle Res. Cell Motil.* **18**, 17–30.
55. Svoboda, K. & Block, S. M. (1994) *Annu. Rev. Biophys. Biomol. Struct.* **23**, 247–285.
56. Veigel, C., Bartoo, M. L., White, D. C., Sparrow, J. C. & Molloy, J. E. (1998) *Biophys. J.* **75**, 1424–1438.
57. Mehta, A. D., Finer, J. T. & Spudich, J. A. (1997) *Proc. Natl. Acad. Sci. USA* **94**, 7927–7931.
58. Barclay, C. J. (1998) *J. Muscle Res. Cell Motil.* **19**, 855–864.